Web Ecol., 26, 251–269, 2026
https://doi.org/10.5194/we-26-251-2026
© Author(s) 2026. This work is distributed under
the Creative Commons Attribution 4.0 License.

eef Web Ecology Open Access

Impacts of climate change on the wild olive (*Olea europaea* subsp. *europaea* var. *sylvestris*) in the Mediterranean Basin

Wisse Zijlstra[1], **Andros Solakis-Tena**[2], **and Noelia Hidalgo-Triana**[1]

[1]Department of Botany and Plant Physiology, University of Málaga, Málaga, 29010, Spain
[2]European Topic Centre, University of Málaga, Málaga, 29010, Spain

Correspondence: Wisse Zijlstra (wiszijlstra@gmail.com)

Received: 14 January 2026 – Revised: 7 October 2026 – Accepted: 12 October 2026 – Published: 3 November 2026

Abstract. Climate change is expected to affect the distribution of Mediterranean plant species, including *Olea europaea* var. *sylvestris* (wild olive), a keystone species for regional biodiversity and an important genetic resource for cultivated olives. Understanding how its range may shift under future climatic conditions is therefore critical for both conservation planning and the resilience of the species. In this study, an ensemble species distribution model combining generalised linear models, generalised additive models, and maximum entropy was used to assess the current and future climatic suitability of *O. europaea* var. *sylvestris* across the Mediterranean Basin under two Shared Socioeconomic Pathway climate change scenarios: SSP2–4.5 and SSP5–8.5. A total of 558 verified presence records were compiled, including 479 records obtained from the Global Biodiversity Information Facility and 79 records from regional herbaria, and combined with six bioclimatic variables. These variables were selected based on their ecological relevance and supported by Pearson correlation analysis. Current projections indicate high habitat suitability in the Iberian Peninsula, southern Italy, North Africa, and coastal areas where suitability persists across scenarios. However, all future projections reveal a reduction in suitable area, most pronounced under SSP5–8.5 for the period 2061–2080, accompanied by a clear northward shift in favourable habitat. These findings demonstrate that future climatic conditions are likely to substantially reduce the climatic suitability of *O. europaea* var. *sylvestris*, thereby increasing its ecological vulnerability. Reducing greenhouse gas emissions and promoting sustainable land management remain essential to slowing the pace of habitat loss and supporting the long-term persistence of wild olive populations.

1 Introduction

Climate change represents a major threat to biodiversity and ecosystem functioning worldwide (Gulev et al., 2021). It alters temperature and precipitation patterns, and increases the frequency of extreme weather events, which disrupt ecological processes and drive shifts in species distributions. Plant communities are especially vulnerable, as they may experience reduced habitat suitability and altered ecological interactions, including pollination, water regulation, and soil stability (Pecl et al., 2017). Furthermore, climate-change-induced shifts can increase dry, desert-like conditions, directly impacting plant species through altered phenology and range shifts, often towards higher altitudes or latitudes (Rubenstein et al., 2023). Reduced water availability, heightened erosion, nutrient loss, and more frequent droughts and heatwaves can suppress plant growth, increase mortality, reduce genetic diversity, and promote the spread of invasive species (Menezes-Silva et al., 2019).

The Mediterranean Basin is considered one of the most vulnerable regions to climate change, with rising temperatures and altered precipitation patterns threatening its characteristic ecosystems (Cramer et al., 2020). In this context, *Olea europaea* L., which occurs as wild populations in native Mediterranean forests and also includes one of the most widely cultivated tree crops in this region, serves as a valuable bioindicator for assessing the ecological and agricultural consequences of climatic shifts. According to Flora Iberica

(Vargas and Talavera, 2012), this species comprises two varieties: the cultivated *O. europaea* var. *europaea* and the wild *O. europaea* var. *sylvestris* (Mill.) Lehr, commonly known as oleaster. The wild form is native to the Mediterranean Basin and typically grows as a small tree or large shrub with narrow, leathery leaves and thorny basal shoots. Its small, bitter fruits are generally unpalatable and adapted for bird dispersal. In contrast, the cultivated olive has broader leaves, lacks thorns, and produces larger, more palatable fruits selected for oil yield. Despite these differences, both varieties are fully interfertile, and hybridisation is common where wild and cultivated populations coexist or where groves are abandoned (Ben-Dor et al., 2024). Distinguishing between cultivated olives and oleaster fruits can be achieved through ecological, morphological, and genetic criteria (Besnard et al., 2018).

In recent years, species distribution models (SDMs) have become essential tools for assessing the current and future potential distribution of plant species under changing climatic conditions (Miller, 2010). These models provide valuable insights into habitat suitability and are widely applied in conservation strategies and agricultural planning. Among these, the maximum entropy (MaxEnt) algorithm is particularly valued for its strong predictive performance when using presence-only data and limited occurrence records (Phillips et al., 2006; Valavi et al., 2021). There are various climate modelling frameworks for projecting future species distributions. CMIP6 is the latest framework of coordinated global climate model experiments, providing standardised projections under different emission and socioeconomic scenarios, called Shared Socioeconomic Pathways (SSPs), used by the IPCC. SSPs combine greenhouse gas trajectories with socioeconomic narratives that span a wide range of futures. At the very low end, SSP1–1.9 represents a strong sustainability pathway with stringent mitigation measures consistent with limiting warming to around 1.5 °C in line with the Paris Agreement, whereas SSP1–2.6 also follows a sustainable trajectory but allows warming closer to 2 °C. Intermediate scenarios include SSP2–4.5, a "middle-of-the-road" pathway with moderate mitigation, and SSP4–6.0, which reflects a world of deep inequalities combined with medium-high emissions. High-emission scenarios include SSP3–7.0, characterised by regional rivalry and significant challenges to both mitigation and adaptation; and SSP5–8.5, a fossil-fuel-intensive development pathway that leads to very high emissions and warming exceeding 4 °C by 2100 (O'Neill et al., 2016). Including multiple models and scenarios is essential for accounting for uncertainty in future climate projections and producing robust ecological insights.

In this study, we assess the potential impact of climate change on the current and future distribution of *O. europaea* var. *sylvestris* using SSP2–4.5 (stabilisation pathway) and SSP5–8.5 (high-emission pathway) to capture intermediate and extreme futures. Unlike most previous studies limited to national or regional scopes, this research covers the entire Mediterranean Basin.

The objectives of this study are (1) to evaluate the predictive performance of the ensemble model for *O. europaea* var. *sylvestris* and identify the climatic variables most strongly influencing its current distribution, (2) to analyse climatic preferences and tolerance thresholds using response curves, (3) to map its current habitat suitability under present climate conditions, and (4) to project and quantify future changes in the distribution of suitable areas under SSP2–4.5 and SSP5–8.5 for the mid-century (2041–2060) and late-century (2061–2080) periods.

2 Material and methods

2.1 Study area

The Mediterranean Basin is recognised as a global biodiversity hotspot, characterised by a Mediterranean climate with hot, dry summers and mild, wet winters (Médail and Quézel, 1999). The region encompasses diverse landscapes, including coastal areas, mountain ranges, and semi-arid environments. This study adopts the Mediterranean region boundary defined by Olson et al. (2001), with a slight modification. A small part of north-west Spain was included, and the Canary Islands were excluded because the region has a subtropical climate (Luque Söllheim et al., 2024). The study area map was generated in QGIS v3.40.8 (EPSG:4326) (Fig. 1).

2.2 Species occurrence data

A total of 1283 presence records for *O. europaea* var. *sylvestris* were obtained from the Global Biodiversity Information Facility (GBIF, 2025). Only herbarium-preserved specimens were included to ensure data quality, as these records are based on physical plant material that has been collected and preserved, such as specimens pressed and affixed to herbarium sheets. Observational records lacking physical specimens were excluded. To ensure comprehensive coverage, the search in GBIF included several taxonomic synonyms listed in Plants of the World Online (POWO, 2025), an authoritative global database of accepted plant names and synonyms. The search terms included *O. sylvestris* Mill., *O. europaea* var. *sylvestris* (Mill.) Lehr, *O. europaea* subsp. *sylvestris* (Mill.) Rouy, *O. europaea* subsp. *sylvestris* (Mill.) Rouy ex Hegi, and *O. europaea* subsp. *europaea* (GBIF.org, 2025). To complement GBIF data, 170 herbaria listed in the Index Herbariorum (Sweetgum, 2025) and located within the Mediterranean Basin were contacted by email, coordinated through the Herbarium of the University of Málaga (MGC). From the herbaria that replied, 13 provided usable records for *O. europaea* var. *sylvestris*, yielding 422 records, of which 79 were retained after cleaning.

Each record was reviewed to confirm that it represented wild, non-cultivated individuals, using contextual information such as location, habitat type, and collection notes. Records from botanical gardens or clearly cultivated settings

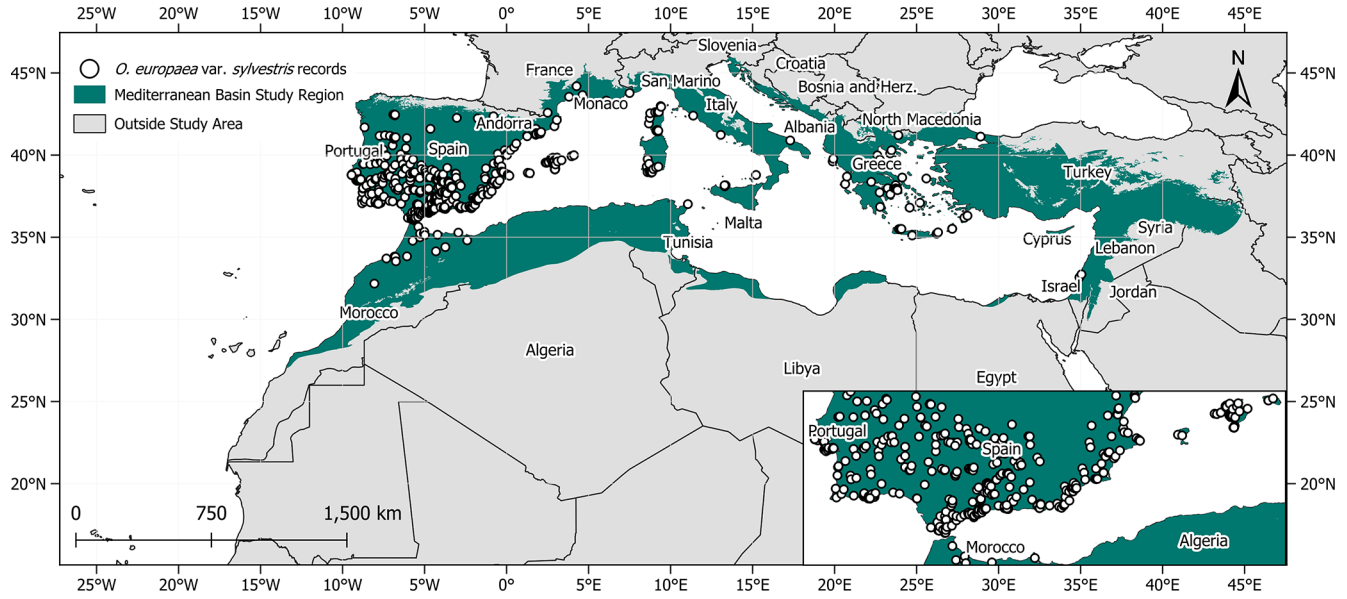


Figure 1. Map of the Mediterranean Basin (EPSG:4326) showing the study area and the occurrence records of *Olea europaea* var. *sylvestris* (white points). Map created by the authors based on Olson et al. (2001), with occurrence data from GBIF.org (2025) and regional herbaria.

were excluded. Complementary data provided by herbaria were checked for duplication against GBIF data, and duplicates were removed.

Occurrence records were not spatially thinned because the final cleaned dataset contained a limited number of unique, verified presence points; applying even a moderate thinning distance would have substantially reduced the sample size and weakened the model's ability to characterise the species' environmental niche. As a consequence, the model remains sensitive to spatial sampling bias, with a risk of overfitting and overestimated suitability near densely sampled areas such as the Iberian Peninsula (see Sect. 4.5). Some records lacked precise coordinates; therefore, when possible, coordinates were estimated from locality descriptions. All occurrences were georeferenced, checked for spatial accuracy in QGIS version 3.40.8 (QGIS Association, 2025), and verified against the Mediterranean Basin boundary map (Fig. 1). After data cleaning, 479 of the 1283 GBIF records and 79 of the 422 herbarium records were retained for modelling, resulting in a total of 558 occurrence records.

2.3 Bioclimatic data

We obtained 19 bioclimatic variables from WorldClim v2.1 at 30 arcsec ($\sim 1\,\mathrm{km}^2$; Fick and Hijmans, 2017) resolution, representing historical averages from 1970 to 2000. Descriptions of these variables (bio1–bio19) are provided in Table A1.

Future projections for 2041–2060 and 2061–2080 were derived from the CMIP6 model EC-Earth3-Veg (Döscher et al., 2022) under the SSP2–4.5 and SSP5–8.5 scenarios (O'Neill et al., 2016). This model was selected for its demonstrated accuracy in simulating European climates (Filahi et al., 2025). SSP2–4.5 (intermediate development with moderate emissions) and SSP5–8.5 (fossil-fuel-driven growth with very high emissions) were used to capture a range of plausible mid- and late-century climate futures, from intermediate to more extreme warming trajectories. Projections were limited to the 2041–2060 and 2061–2080 periods to emphasise short- and medium-term changes in habitat suitability.

All 19 bioclimatic variables were clipped to the study area (Fig. 1) using the translate tool of QGIS v3.40.8. Since using too many predictors can reduce model performance and transferability, and increase the risk of overfitting, particularly when highly correlated variables are included, we reduced the variable set to those most relevant, as recommended in Elith et al. (2011). Multicollinearity among climatic variables was assessed using Pearson correlations in R v4.5.1. Analyses were run in RStudio v2025.5.1.513 (Posit Team, 2025). Following recommendations on handling collinearity in distribution models (Dormann et al., 2013), variables with a Pearson correlation coefficient $|r| > 0.75$ were considered highly correlated, and one variable from each correlated pair was excluded from further analysis. The final set of six predictors was selected on the basis of the Pearson correlation analysis and the ecological relevance of each variable, and these variables were then used directly in all three algorithms (GLM, GAM, and MaxEnt).

2.4 Species distribution modelling

Species distribution models (SDMs) were developed using the advanced ensemble modelling framework biomod2

(Guéguen et al., 2026) combined with the terra package for optimised spatial data processing within the R environment. To characterise the environmental profile of the species, a multi-algorithm approach was implemented, combining regression techniques and machine learning algorithms: generalised linear models (GLMs; Nelder and Wedderburn, 1972), generalised additive models (GAMs; Wood, 2017), and maximum entropy (MaxEnt v. 3.4.4; Phillips et al., 2025). MaxEnt modelling was executed natively by integrating the maxent.jar application via the dismo Java interface on R. Feature classes were left at the automatic MaxEnt setting, which for the training sample size enabled linear, quadratic, product, hinge, and threshold features. To account for the absence of true absence data, a background selection strategy was adopted. A single pool of 10 000 pseudo-absences (PAs) was randomly generated across the study area. For GLM and GAM algorithms, automated formula and hyperparameter selection native to biomod2 were used to prevent artificial overfitting.

Occurrence data comprised presence records from GBIF and the additional herbarium sources described earlier. Historical bioclimatic variables (1970–2000) were used as the baseline conditions, whereas future climate variables for both SSPs and time periods served as projection layers. Model performance and predictive robustness were assessed using a repeated split-sample cross-validation scheme. For each algorithm, the dataset was randomly split into 10 independent evaluation replicates, generated using 25 % of occurrence points for testing and 75 % for training, with a random seed set for reproducibility. Model accuracy was evaluated using the area under the curve (AUC) of the receiver operating characteristic (ROC) curve (Pontius and Parmentier, 2014) and the true skill statistic (TSS) metrics (Allouche et al., 2006), with a default prevalence of 0.5. AUC values range from 0 to 1, where 0.5 indicates a model performing no better than random and 1.0 indicates perfect discrimination (Fielding and Bell, 1997). To minimise individual algorithmic biases and reduce structural uncertainty, an ensemble model (EM) consensus was built by combining all calibrated individual models and cross-validation runs into a single global consensus framework. To ensure predictive quality, only individual models achieving a TSS score greater than or equal to 0.4 were retained for the ensemble assembly. Final potential suitability maps for both baseline (current) and future environmental scenarios were projected across the spatial grid and converted onto a standardised continuous scale ranging from 0 (completely unsuitable) to 1000 (maximum suitability).

Full documentation of the modelling workflow following the ODMAP protocol (Zurell et al., 2020) is provided in Appendix D.

In addition, predictor influence was evaluated via a permutation-based variable importance procedure executed with three repetitions per model run. In biomod2, this is calculated as $1-r$ between the reference prediction and the prediction obtained after randomly permuting each predictor in turn, computed independently for each variable. The resulting values therefore express the influence of each predictor separately and are not shares of a common total, so they do not sum to 100. Therefore, model outputs were used to identify the most influential climatic variables to generate current and future habitat suitability maps and to visualise potential shifts in the geographic distribution of *O. europaea* var. *sylvestris*. Final suitability maps were based on the EM output (0–1000) across the 30 replicates (10 runs with GLM, GAM, and MaxEnt) to ensure robust prediction and reduced sensitivity to sampling variability (Phillips et al., 2006; Elith et al., 2011).

For clarity in interpretation and spatial analysis, the continuous suitability output was rescaled from 0–1000 to 0–1 and reclassified into five equal-interval habitat suitability classes of 0.2 width: unsuitable ($p < 0.2$), low ($0.2 \leq p < 0.4$), moderate ($0.4 \leq p < 0.6$), high ($0.6 \leq p < 0.8$), and very high ($p \geq 0.8$). The class boundaries are equal intervals adopted for presentation and area-based comparison, not ecological thresholds, following classification schemes commonly used in ecological modelling studies (Li et al., 2020; Khan et al., 2022; Alegria et al., 2023). This classification enhanced the visualisation of habitat patterns, enabled comparison across scenarios, and facilitated the area-based analysis of habitat shifts under projected climate conditions. To quantify habitat suitability under current and future climate scenarios, the classified suitability rasters were processed in R using the terra package (Hijmans, 2025). For each raster, the number of cells per suitability class was extracted using the freq() function, and the area of each class was calculated by multiplying the cell count by the pixel area, derived from the raster resolution using the res() function. For area calculation, the classified rasters were reprojected to a cylindrical equal-area projection, giving a cell size of approximately 739.59 m × 739.59 m, so that each pixel corresponded to approximately 0.547 km^2. The resulting areas (km^2) were computed for all scenarios to allow quantitative comparison of habitat suitability, expressed as the estimated area within each suitability class across different time periods and climate conditions.

3 Results

3.1 Bioclimatic variables and model performance

Six bioclimatic variables were retained on the basis of low intercorrelation ($|r| < 0.75$) (Fig. A1), and ecological relevance to the distribution of *O. europaea* var. *sylvestris* in Mediterranean climates. The relative permutation importance of these variables is summarised in Table 1. Minimum temperature of the coldest month (bio6) showed the highest permutation importance. Mean temperature of the warmest quarter (bio10) had the second-highest permutation importance, whereas precipitation of the warmest quarter (bio18)

Table 1. Permutation importance of the six bioclimatic variables used in the ensemble model for *Olea europaea* var. *sylvestris*, averaged across the GLM, GAM, and MaxEnt single models.

Code	Climatic variable	Permutation importance
bio6	Minimum temperature of coldest month	64.9
bio10	Mean temperature of warmest quarter	30.9
bio18	Precipitation of warmest quarter	11.1
bio15	Precipitation seasonality (coefficient of variation)	9.0
bio12	Annual precipitation	8.8
bio2	Mean diurnal range (mean monthly max–min)	4.0

indicated the third-highest permutation importance (complete information of permutation importance by algorithm can be found in Table S1 in the Supplement).

Using these six variables, the ensemble model revealed strong predictive performance, with a mean calibration AUC of 0.9 and a mean calibration TSS of 0.7 (Fig. B1), along with a sensitivity of 87.4 % and a specificity of 79.3 %. Performance on the held-out validation data was comparable for AUC and slightly lower for TSS, indicating good discrimination with little overfitting. The ROC curve indicated good discrimination (mean AUC = 0.9), well above random expectation (AUC = 0.5).

3.2 Analysis of climatic variables

The response curves (Fig. 2; complete information in Table S2) show the relationship between environmental variables and the predicted suitability of *O. europaea* var. *sylvestris*, outlining the climatic ranges associated with higher suitability. For bio2 (mean diurnal range), suitability was lowest at approximately 7.5 °C and then rose with increasing values, reaching its highest values at the upper end of the observed range (approximately 16 °C). Bio6 (minimum temperature of coldest month) revealed unsuitable ($p < 0.2$) conditions where temperatures were below approximately 0.5 °C, with a sharp increase above 1.5 °C and the highest suitability at approximately 9 °C. For bio10 (mean temperature of warmest quarter), suitability began to increase at approximately 16 °C and reached its peak at 20 °C, followed by a steep decline beyond 24 °C, becoming unsuitable at temperatures over 25 °C.

Bio12 (annual precipitation) was associated with maximum suitability of around 500 mm, with a decline on both sides of this peak, with unsuitable conditions below 300 mm and above 1250 mm of annual precipitation (Table S2). Bio15 (precipitation seasonality) had a pronounced peak at a coefficient of variation of about 50, followed by a decline and a moderate secondary rise near 110. Bio18 (precipitation of the warmest quarter; Fig. 2) rose steeply from 0 mm to a peak at approximately 30 mm, declined to a plateau by approximately 75 mm, and remained within the low-suitability class across the remainder of its range, with a secondary rise near 175 mm. Suitability did not fall below 0.2 at any point across the observed range of this variable.

3.3 Current suitable distribution

Under current climatic conditions, large parts of the Iberian Peninsula, particularly southern and central Spain and Portugal, exhibited extensive areas of high to very high suitability for *O. europaea* var. *sylvestris* (Fig. 3). Southern Italy; the western coastal zones of Greece, northern and central Morocco; and parts of Algeria and Tunisia also revealed considerable suitable habitat. Smaller but distinct patches of suitability were found on Mediterranean islands such as Sicily, Corsica, and Crete, as well as along coastal fringes of the Mediterranean Levant, including parts of Lebanon and Palestine.

3.4 Future distribution and suitable changes

In this section a classified categorical map is shown (Fig. 4). The map shows five suitability classes: unsuitable (< 0.2), low (0.2–0.4), moderate (0.4–0.6), high (0.6–0.8), and very high (≥ 0.8), under the current (Fig. 4a) and future (Fig. 4b–e) conditions. To check the continuous suitability maps, see Fig. C1 in Appendix C. Using the six selected bioclimatic variables, projections for 2041–2060 and 2061–2080 under SSP2–4.5 and SSP5–8.5 revealed consistent shifts in habitat suitability (Fig. 4b–e). All future scenarios indicated a reduction in total suitable area and a general northward shift in optimal habitat, particularly across northern Spain, southern France, northern and central Italy, and parts of Greece and Türkiye. Under SSP2–4.5, both 2041–2060 (Fig. 4b) and 2061–2080 (Fig. 4c) displayed broadly similar patterns in suitability and range shift, with moderate contraction of highly suitable areas. SSP5–8.5 for 2041–2060 (Fig. 4d) showed a comparable pattern, but SSP5–8.5 for 2061–2080 (Fig. 4e) resulted in a much stronger loss of highly suitable habitat.

Many areas classified as highly or very highly suitable under current conditions were downgraded to lower-suitability categories or became unsuitable, especially in the southern Mediterranean regions. However, some coastal areas, including parts of Portugal, northern Morocco, and parts of Spain, persisted as isolated hotspots of high or very high suitability. Portugal retained relatively high suitability across all future projections.

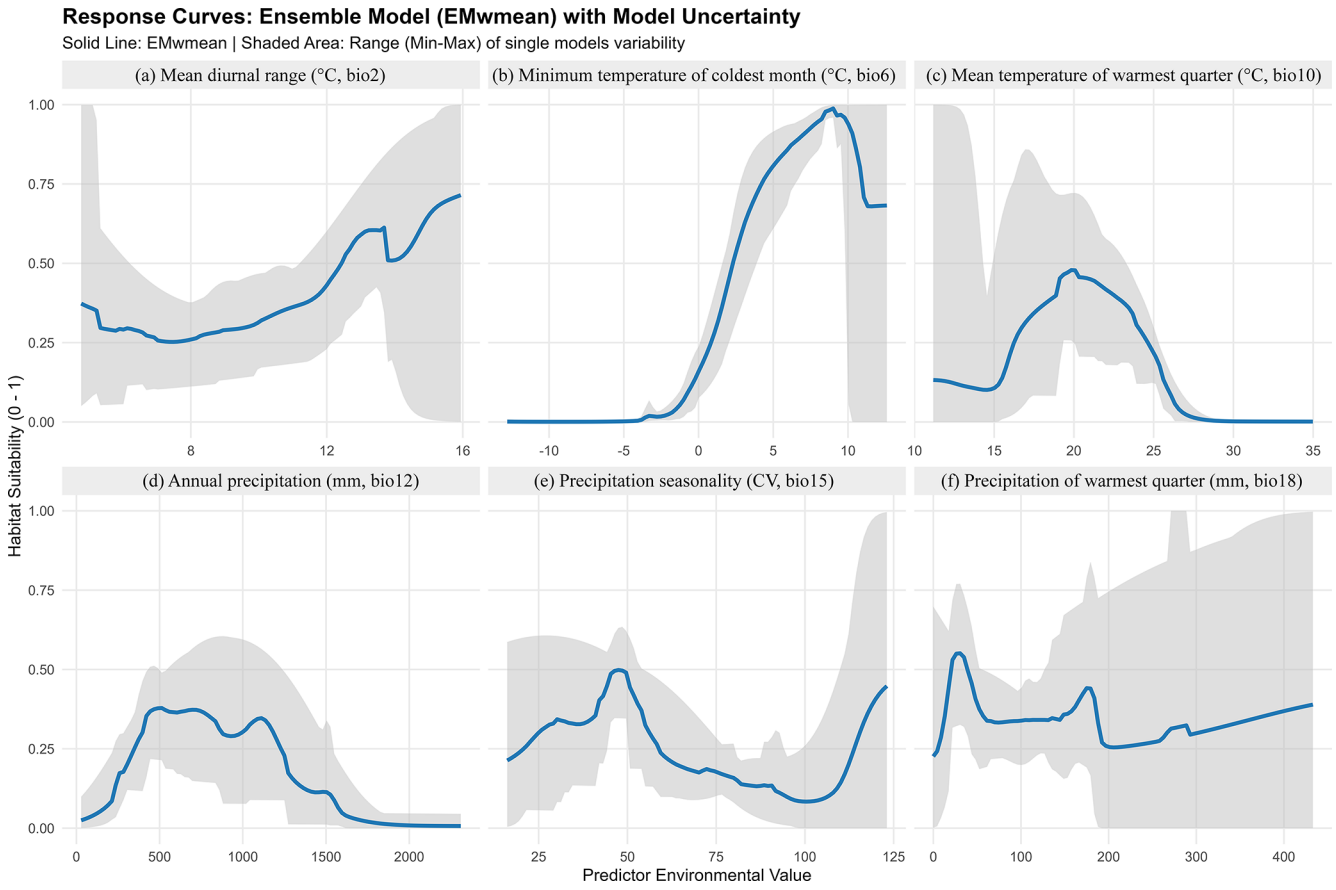


Figure 2. Predicted response curves from the ensemble weighted mean model (EMwmean), showing uncertainty from all single models. The response curves show the predicted suitability for *Olea europaea* var. *sylvestris* changes across the range of each bioclimatic predictor, while all other predictors are held at their mean values. The curves represent the model-estimated change in the likelihood of presence in response to each predictor, not a directly measured biological response of the species: (bio2) mean diurnal range (°C), (bio6) minimum temperature of the coldest month (°C), (bio10) mean temperature of the warmest quarter (°C), (bio12) annual precipitation (mm), (bio15) precipitation seasonality (CV), and (bio18) precipitation of the warmest quarter (mm). The blue lines indicate the mean values, whereas grey areas denote the minimum–maximum range across the cross-validation and algorithm runs.

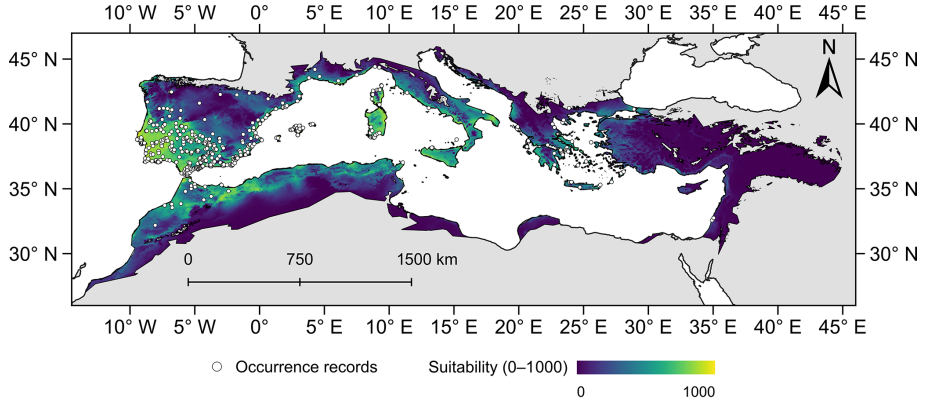


Figure 3. Predicted current continuous habitat suitability map (0–1000) for *Olea europaea* var. *sylvestris* under present-day climate conditions with the records overlaid.

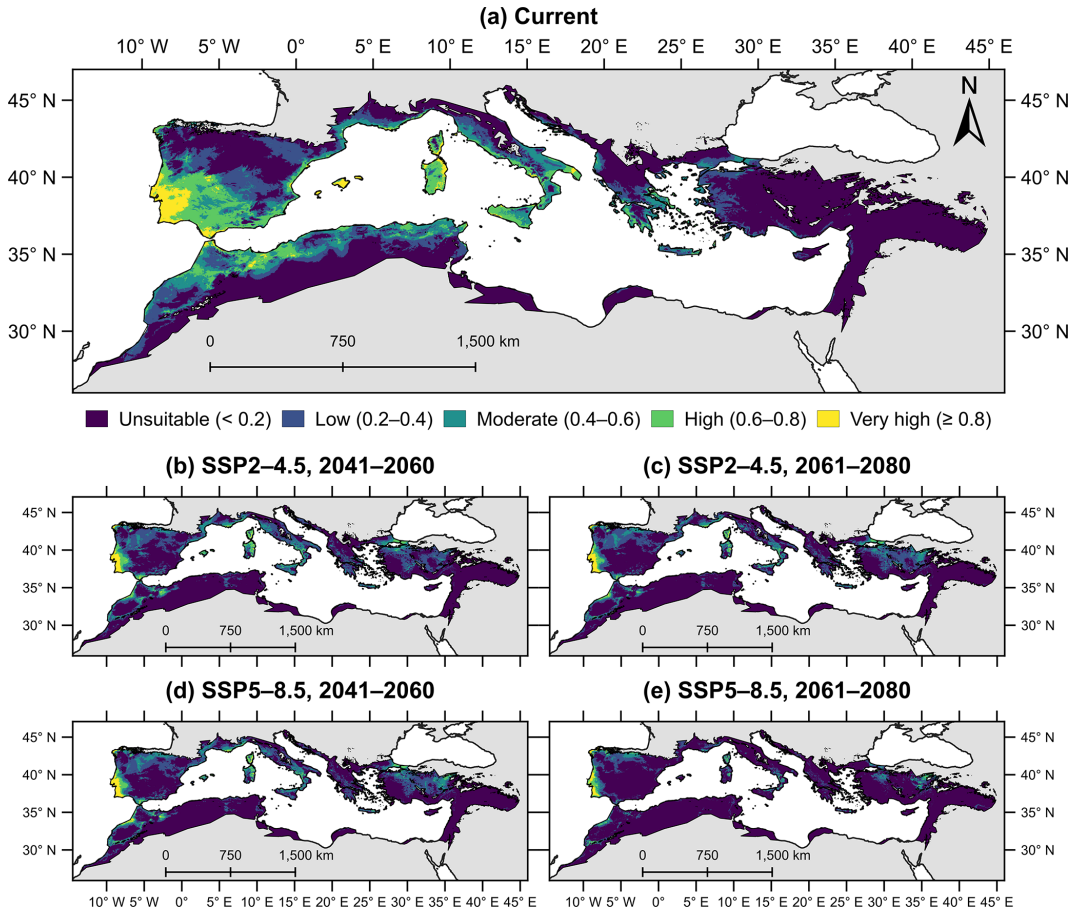


Figure 4. Predicted habitat suitability maps for *Olea europaea* var. *sylvestris* under **(a)** present-day climate conditions; and future climate scenarios: **(b)** SSP2–4.5 for 2041–2060, **(c)** SSP2–4.5 for 2061–2080, **(d)** SSP5–8.5 for 2041–2060, and **(e)** SSP5–8.5 for 2061–2080. Suitability classes: unsuitable ($p < 0.2$), low ($p = 0.2 - 0.4$), moderate ($p = 0.4 - 0.6$), high ($p = 0.6 - 0.8$), and very high ($p \geq 0.8$).

3.5 Projected changes in habitat suitability area

Table 2 summarises the estimated area ($\times 10^4\,\mathrm{km}^2$) under each suitability class for current and future scenarios. All future projections show a decline in the area classified as moderately, highly, or very highly suitable compared with current conditions. The SSP5–8.5 scenario for 2061–2080 showed the most pronounced decline, with a strong increase in the area classified as unsuitable and a marked reduction in high and very high suitability classes, suggesting a substantial loss of climatically suitable habitat for *O. europaea* var. *sylvestris* by the end of the century. Highly suitable area (≥ 0.6) declined from $29.7 \times 10^4\,\mathrm{km}^2$ under current conditions to $5.3 \times 10^4\,\mathrm{km}^2$ under SSP5–8.5 for 2061–2080, a reduction of more than 80 %.

4 Discussion

4.1 Model performance

Only ecologically meaningful and non-redundant bioclimatic predictors were retained, which improves model interpretability, reduces overfitting, and enhances transferability (Phillips et al., 2006; Elith et al., 2011). The resulting model achieved a mean calibration AUC of 0.9 and a TSS of 0.7, indicating good discrimination between suitable and unsuitable conditions. This value is unlikely to be much higher for a broadly distributed taxon, as previous work has shown that species with wide geographic ranges often exhibit lower AUC scores because it is more difficult for the model to distinguish suitable from unsuitable habitat across diverse environments (McPherson and Jetz, 2007).

4.2 Climatic drivers of habitat suitability

In this study, bio6 (minimum temperature of the coldest month) and bio10 (mean temperature of the warmest quarter) emerged as key contributors to habitat suitability for *O. eu-*

Table 2. Area ($\times 10^4$ km^2) under each habitat suitability class for each climate scenario.

Suitability class	Current	SSP2–4.5 (2041–2060)	SSP2–4.5 (2061–2080)	SSP5–8.5 (2041–2060)	SSP5–8.5 (2061–2080)
Unsuitable (< 0.2)	142.5	160.4	169.5	163.0	203.4
Low (0.2–0.4)	41.2	51.7	47.2	49.7	24.7
Moderate (0.4–0.6)	28.5	19.6	17.2	19.6	8.4
High (0.6–0.8)	23.4	7.4	5.3	6.6	3.8
Very high (≥ 0.8)	6.3	2.8	2.6	3.0	1.6
Total suitable (0.2–1)	99.4	81.5	72.4	78.9	38.5
Highly suitable (≥ 0.6)	29.7	10.2	8.0	9.6	5.3

ropaea var. *sylvestris*, underlining the importance of temperature extremes in shaping its distribution. This is consistent with the physiology of *O. europaea*: minimum winter temperatures directly affect survival and seedling recruitment, as freezing conditions can cause cold stress and mortality (Petruccelli et al., 2022; Ruiz et al., 2006), whereas excessively high summer temperatures can impair photosynthesis and fruit development, limiting reproductive success in overly hot environments (Haworth et al., 2018).

Together, these two thermal variables exert opposing pressures on the species' projected distribution under a future climate. Warming winter minima (bio6) make previously too-cold areas to the north and at higher elevations newly suitable, driving the northward and upslope shifts seen across the projections. At the same time, rising summer temperatures (bio10) push the warmer, low-elevation, and inland parts of the current range beyond the species' heat tolerance threshold, rendering them unsuitable. Because bio10 warming affects a substantially larger portion of the current range than the area newly opened by bio6 warming, the net outcome is a pronounced loss of suitable habitat. In other words, more of the currently suitable range becomes too hot in summer than is gained from milder winters in newly suitable areas farther north and upslope, which explains both the northward shift and the overall reduction in suitable area found in this study. A similar pattern has been reported for olive elsewhere in the Mediterranean. Özdel et al. (2025) projected a northward and upslope redistribution for cultivated olive in Türkiye, with the high-suitability class contracting sharply (from 4.4 % to 0.2 % of the country under SSP5–8.5 by 2081–2100) even as lower-suitability classes expanded, and Arenas-Castro et al. (2020) reported net reductions in suitability for olive varieties in southern Spain. Our basin-wide results for the wild variety show a comparable direction of poleward displacement, although the underlying species, extent, and predictors differ between studies. Precipitation of the warmest quarter (bio18) was also an important variable influencing modelled habitat suitability. This aligns with other studies (Arenas-Castro et al., 2020). In their assessment of climate change impacts on olive varieties, including *O. europaea* var. *sylvestris*, Arenas-Castro et al. reported that changes in water availability driven by decreasing precipitation and increasing evapotranspiration were the dominant factors reducing future suitability. They found that much of the projected loss of suitable area was associated with drier conditions, especially in autumn.

The response curve in bio15 seems to highlight the strong dependency of *O. europaea* var. *sylvestris* on Mediterranean precipitation seasonality regimes. The primary predictive optimum (at a coefficient of variation of ~ 50) aligns with the balanced climate conditions of the Mediterranean Basin where the species is ecologically and climatically dominant. The species being a sclerophyll, the first peak fits the Mediterranean climatic adaptation of *O. europaea* var. *sylvestris* (Guerrero Maldonado et al., 2016). Conversely, the secondary moderate rise observed at high seasonality values (~ 110) suggests the species' capacity to persist under scenarios of extreme intra- or inter-annual climate variability, indicating tolerance of highly seasonal eastern Mediterranean climates. However, this secondary peak may also indicate an artefact of sparse and spatially uneven occurrence data. Given the wider uncertainty around this part of the curve, the secondary peak should be interpreted cautiously.

Although factors such as soil properties, topography, and grazing pressure may also influence wild olive distribution (Tsiftsis et al., 2025), this study intentionally focuses on climatic suitability as a standalone driver.

4.3 Species distribution data and current suitability

Suitability tends to be lower in inland, mountainous, or more arid regions, where colder winter temperatures and reduced water availability are likely to constrain the species' distribution. Large portions of the eastern Mediterranean, such as Syria and inland regions of Türkiye, are predicted to be unsuitable, although these predictions should be interpreted cautiously given the absence of occurrence data from these regions, as discussed in the limitations.

It is not always possible to determine whether each occurrence record truly represents the wild form *O. europaea* var. *sylvestris* because many collectors and databases record specimens simply as *O. europaea* without specifying the variety. This uncertainty is reinforced by the fact that *O. eu-*

ropaea var. *sylvestris* (Mill.) Lehr is currently treated as a synonym of *O. europaea* subsp. *europaea* in major taxonomic sources, such as POWO (2025) and Dimopoulos et al. (2016). Hybridisation between wild and cultivated olives is also widespread, especially in marginal or abandoned agroecosystems such as old olive groves (Ben-Dor et al., 2024), where feral individuals may be misclassified. Countries such as Italy and Greece contributed fewer records than Spain, but their points were relatively well distributed, which supports more reliable predictions in those regions. Overall, Spain, Portugal, Morocco, France, Italy, and Greece provided occurrence data that broadly cover a representative range of bioclimatic conditions.

4.4 Future distributions and possible migration shifts

Under the intermediate climate scenario SSP2–4.5, some regions such as parts of southern France and central Italy are projected to retain moderate suitability, but areas of high suitability retreat from several core regions, including parts of southern Spain and the Maghreb. These patterns are broadly consistent with studies suggesting northward or upslope shifts of Mediterranean taxa in response to warming (Gritti et al., 2006). Projections for 2041–2060 under SSP5–8.5 are similar to those under SSP2–4.5 for 2061–2080, reflecting the relatively modest divergence between the scenarios during mid-century, when projected changes in temperature and precipitation partly overlap. After 2060, however, SSP5–8.5 diverges more strongly, with substantially greater warming and sharper declines in summer precipitation, as shown for the SSP framework by Fuss et al. (2014). This likely explains the pronounced loss of suitable habitat under SSP5–8.5 for 2061–2080.

Across all future projections, many coastal zones remain suitable. Coastal regions in the Mediterranean tend to warm less than inland or mountainous areas, even under high-emission scenarios (El-Samra et al., 2018). This pattern links closely to mean temperature of the warmest quarter (bio10), as sea breeze effects and maritime influence buffer extreme summer temperatures. Coastal areas also often receive higher summer precipitation than nearby inland regions (Curtis, 2019), which relates to the precipitation of the warmest quarter (bio18) and may provide a climatic buffer against the increasingly frequent droughts characteristic of Mediterranean summers. Portugal, along with several other Mediterranean coastal zones, retains areas of high suitability across all future scenarios. The persistence of these areas likely reflects a combination of moderated summer temperatures and comparatively higher summer rainfall. Although a similar geographical signal has been reported for Portugal, where the cultivated form (*O. europaea* var. *europaea*) may remain comparatively resilient under projected climate change (Fraga et al., 2022), this resilience partly reflects irrigation and active grove management. Wild populations lack these interventions and may therefore prove more vulnerable, therefore the comparison indicates a shared climatic signal rather than equivalent resilience. These coastal zones are identified as areas of projected climatic stability rather than validated refugia. The inference rests on the modelled persistence of suitable climate and on maritime buffering of summer temperature and precipitation (El-Samra et al., 2018; Curtis, 2019), not on direct microclimate, demographic, or stress-physiology data from coastal populations of *O. europaea* var. *sylvestris*. Confirming a refugial function will require field validation, including local microclimate data and demographic or genetic monitoring of coastal versus inland populations of the species.

All projected scenarios in this study indicate a net loss of suitable habitat for *O. europaea* var. *sylvestris*. This contrasts with Kassout et al. (2022), who reported increased suitability for the wild olive in Morocco, with the largest suitable area under RCP8.5 in 2070. The most likely reason for this difference is the role of temperature in each model. Both studies included minimum temperature of the coldest month (bio6), but its importance differed greatly: it was the strongest predictor in our ensemble (permutation importance 64.9), whereas it accounted for only 0.6 % of per cent contribution in Kassout et al. (2022). The opposite held for annual precipitation (bio12), which ranked low here (permutation importance 8.8) but dominated their model at 76.7 %. These metrics are not directly comparable in magnitude, as MaxEnt per cent contribution is normalised to sum to 100, whereas biomod2 permutation importance is computed independently per variable; the comparison is therefore one of rank and direction rather than of absolute values. Our basin-wide model is therefore driven mainly by temperature, whereas their model for Morocco is driven mainly by rainfall. This likely reflects the different study areas: across the whole Mediterranean Basin, cold winters limit the species at its northern and inland edges, making bio6 highly informative, while in the Kassout et al. (2022) study, Moroccan winters are rarely cold enough to limit *O. europaea* var. *sylvestris*, so water availability matters more. Because our model is temperature led, warming has two opposing effects: milder winters (bio6) let the species spread northward, while hotter summers (bio10) make southern areas unsuitable; this warm-edge loss outweighs the northern gain, producing a net decline. In a rainfall-driven model where temperature is not limiting, warming does not impose this penalty, so suitability can instead increase. The studies also differ in their climate data (CMIP6 under SSPs here versus CMIP5 under RCPs) and number of predictors (6 versus 12), which can further affect the results. Notably, Kassout et al. (2022) also found declining suitability for the endemic *O. europaea* subsp. *maroccana*. Arenas-Castro et al. (2020), assessing several olive varieties including *O. europaea* L. subsp. *europaea* var. *sylvestris*, reported reduced suitability for six of seven varieties, with marked declines for the wild variety in Spain under the 2040, 2070, and 2100 projections, which agrees with the trends found here.

Furthermore, Hidalgo-Triana et al. (2023) showed that western Mediterranean *O. europaea* var. *sylvestris* forests are highly exposed to climatic change. This corresponds with the strong reduction in suitable areas in the southern Iberian Peninsula found in our study. However, the authors argue that, despite this high exposure, these forests are less vulnerable to climate change because the species possesses functional traits that confer resilience to increasingly dry and hot conditions.

Projections in this study focused on the mid- and late-century horizons (2041–2060 and 2061–2080) to provide more actionable information for conservation planning and management of the species. Longer-term projections could also be informative for assessing potential range collapse or the need for assisted migration under more extreme warming.

4.5 Limitations and caveats

Model output should be interpreted carefully, as it reflects the specific combination of bioclimatic variables used in this study, and a different variable set may cause variations in the distribution patterns. Future projections here rely on a single CMIP6 model; incorporating additional models (for example, IPSL-CM6A-LR and MRI-ESM2-0) would allow between-model climate uncertainty to be quantified and is a priority for further work. At the same time, many records are spatially clustered, for example, in specific parks or forest stands, which can introduce sampling bias and lead to overestimation of suitability near well-sampled locations (Anderson and Raza, 2010; Fourcade et al., 2014). Because the final cleaned dataset contained only 558 unique presence points, spatial thinning was not applied in order to retain sufficient environmental coverage, but this may amplify the effects of clustering. Several Mediterranean countries lacked occurrence data in this study, including Algeria, Tunisia, Palestine, Israel, Lebanon, Syria, and especially Türkiye. This absence does not imply that the species is ecologically absent in these regions. For Türkiye, 28 herbaria were contacted, but no responses were obtained and no herbarium-preserved records were found in GBIF. A similar lack of accessible herbarium data applied to several of the other countries mentioned above. However, *O. europaea* var. *sylvestris* is known to occur naturally throughout the eastern Mediterranean, and multiple studies document its presence in these areas (Fanelli et al., 2022). In fact, the Mediterranean Levantine region is widely considered the centre of origin of the wild olive, from which it spread westwards across the Mediterranean Basin (Besnard et al., 2013; Besnard et al., 2018). Given this, the "unsuitable" predictions there should be interpreted with caution and treated as an artefact of incomplete occurrence sampling rather than a genuine ecological signal. Future iterations of the model would benefit substantially from incorporating herbarium records and field survey data from these under-represented countries, which would likely expand the predicted suitable area eastward and improve model transferability across the full Mediterranean Basin.

To improve future projections and obtain more accurate SDM outputs for the whole Mediterranean Basin, it will be necessary to expand occurrence datasets, particularly by incorporating records from currently under-represented countries.

5 Conclusion

This study showed that *Olea europaea* var. *sylvestris* has a broad but climatically restricted distribution in the Mediterranean Basin and is projected to lose suitable habitat under future climate conditions.

The modelling identified that mostly temperature, but also precipitation, limits the species' range, reflecting its sensitivity to low and high temperatures and drought. These climatic factors capture the dominant climatic constraints shaping its current distribution.

Current suitability maps revealed extensive suitable habitat in the western Mediterranean, although data gaps in several eastern regions likely resulted in under-representation there.

Future projections under both SSP2–4.5 and SSP5–8.5 consistently revealed a contraction and northward shift of suitable habitat, with the greatest losses late in the century under SSP5–8.5. Several coastal zones, particularly in Portugal, Spain, and northern Morocco, are projected to retain relatively high suitability across scenarios.

Appendix A

Table A1. Description of the 19 bioclimatic variables (bio1–bio19) from WorldClim v2.1 used in species distribution modelling. Temperature variables are expressed in °C, precipitation variables in mm, and seasonality variables as a coefficient of variation (CV) or scaled indices, as indicated.

Code	Climatic variable	Unit
bio1	Annual mean temperature	°C
bio2	Mean diurnal range (mean monthly max–min)	°C
bio3	Isothermality (bio2/bio7 × 100)	–
bio4	Temperature seasonality (standard deviation × 100)	°C (×100)
bio5	Max temperature of warmest month	°C
bio6	Min temperature of coldest month	°C
bio7	Temperature annual range (bio5–bio6)	°C
bio8	Mean temperature of wettest quarter	°C
bio9	Mean temperature of driest quarter	°C
bio10	Mean temperature of warmest quarter	°C
bio11	Mean temperature of coldest quarter	°C
bio12	Annual precipitation	mm
bio13	Precipitation of wettest month	mm
bio14	Precipitation of driest month	mm
bio15	Precipitation seasonality (coefficient of variation)	–
bio16	Precipitation of wettest quarter	mm
bio17	Precipitation of driest quarter	mm
bio18	Precipitation of warmest quarter	mm
bio19	Precipitation of coldest quarter	mm

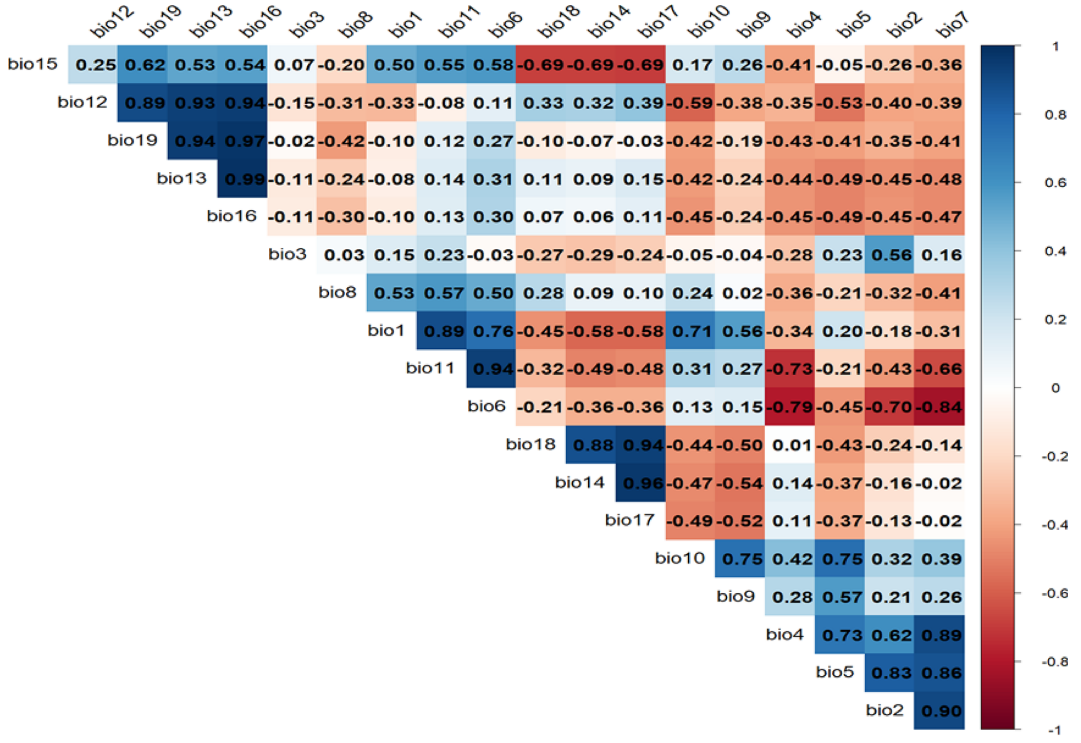


Figure A1. Pearson's correlation matrix of the initially selected 19 bioclimatic variables.

Appendix B

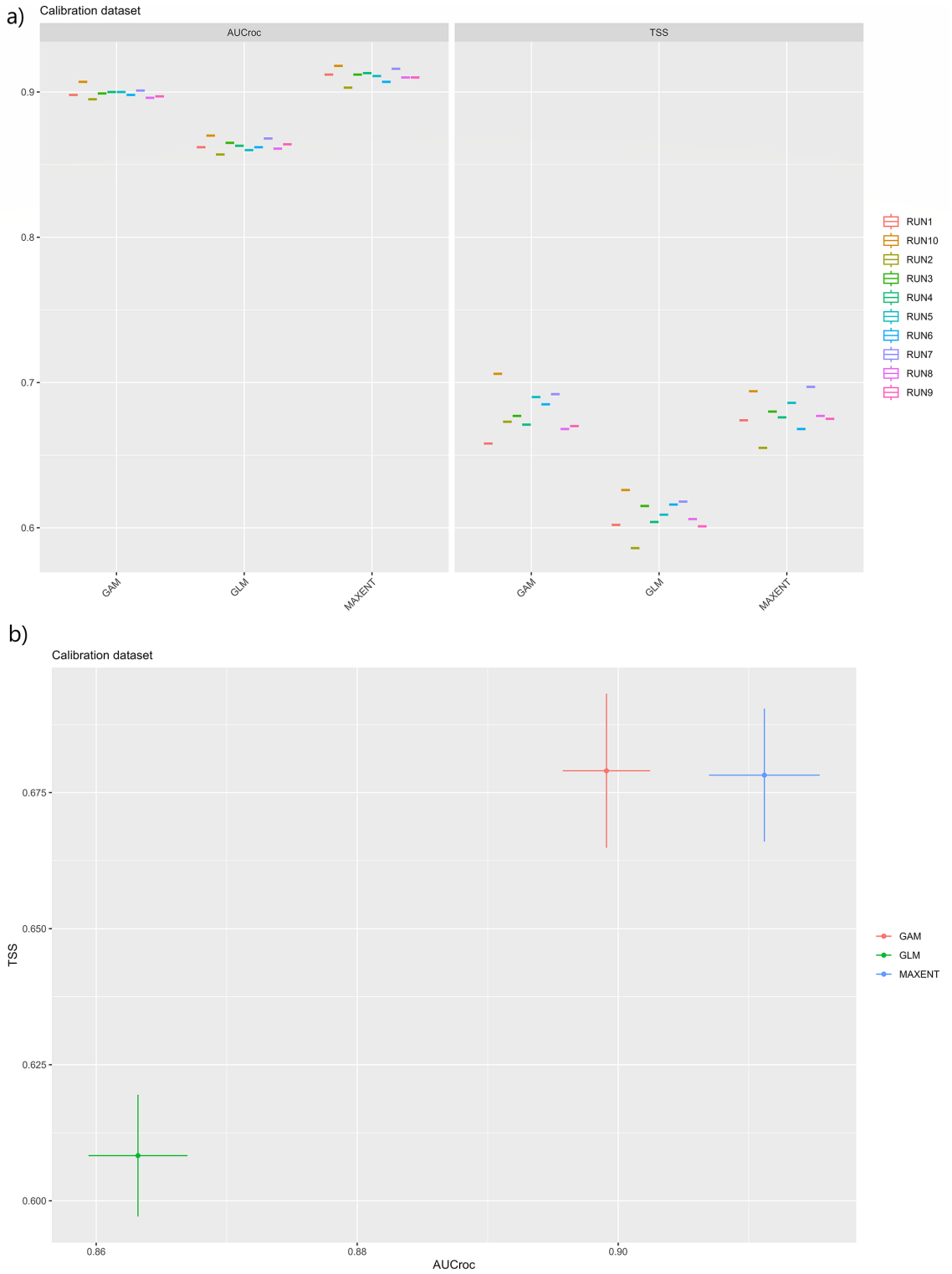


Figure B1. Calibration performance of the single-algorithm models (GLM, GAM, and MaxEnt) across the 30 cross-validation runs, showing the true skill statistic (TSS) and the area under the curve (AUC) of the receiver operating characteristic (ROC) curve: **(a)** individual runs by algorithm, **(b)** mean and standard deviation by algorithm.

Appendix C

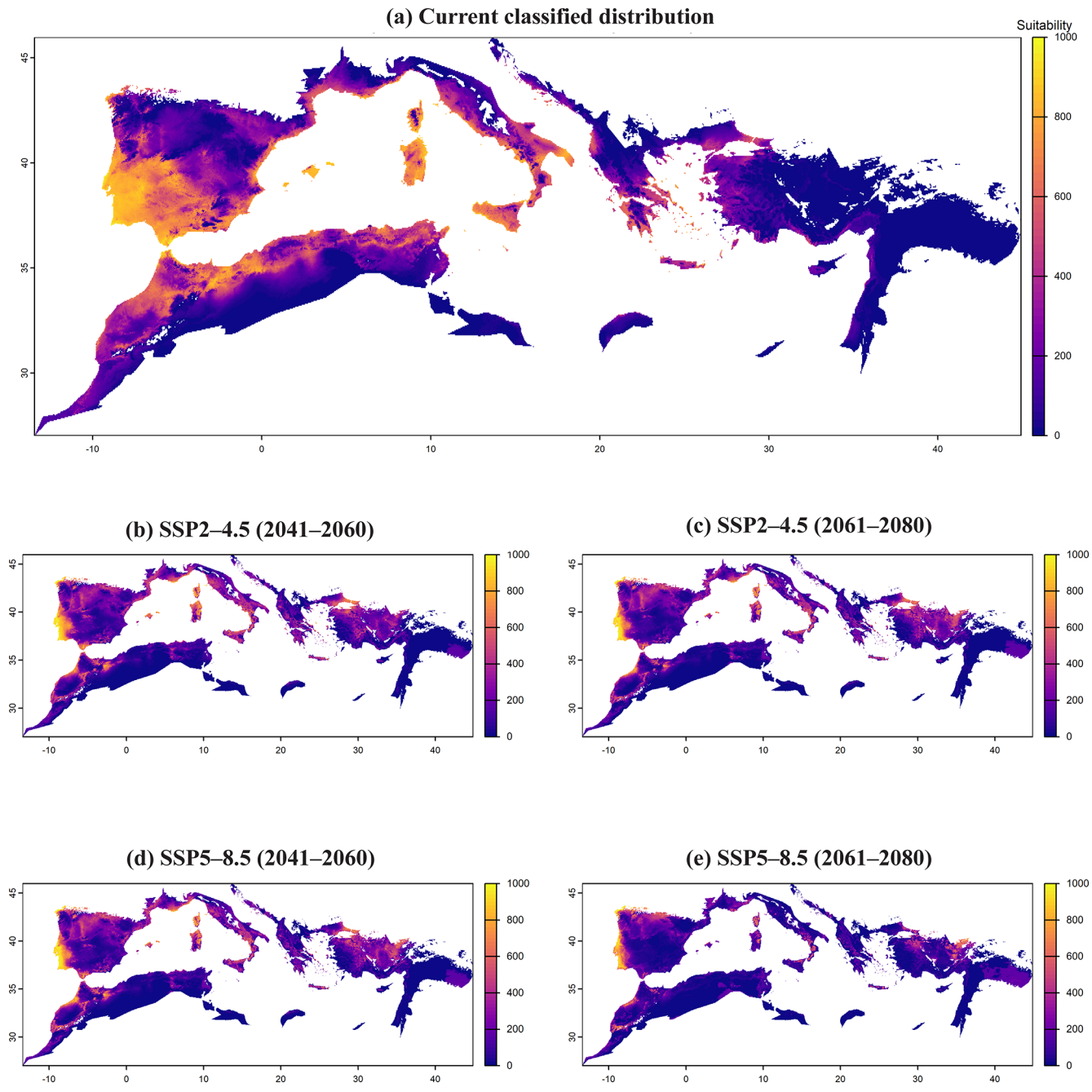


Figure C1. Predicted continuous habitat suitability maps (0–1000) for *Olea europaea* var. *sylvestris* under **(a)** present-day climate conditions, and future climate scenarios: **(b)** SSP2–4.5 for 2041–2060, **(c)** SSP2–4.5 for 2061–2080, **(d)** SSP5–8.5 for 2041–2060, and **(e)** SSP5–8.5 for 2061–2080.

Appendix D

ODMAP protocol (Zurell et al., 2020) documenting the species distribution model for *Olea europaea* var. *sylvestris*.

D1 Overview

D1.1 Objectives

Model objective: forecast and transfer

Target output: continuous habitat suitability index scaled from 0 to 1000

D1.2 Focal taxon

Olea europaea subsp. *europaea* var. *sylvestris* (Mill.) Lehr (wild olive, oleaster)

D1.3 Location

Mediterranean Basin

D1.4 Scale of analysis

Spatial extent: −13.45, 44.92, 27.01, 45.98 (xmin, xmax, ymin, ymax)

Spatial resolution: ∼ 1 km (30 arcsec)

Temporal extent: baseline 1970–2000; projections 2041–2060 and 2061–2080

Temporal resolution: multidecadal climate averages

Boundary: polygon

D1.5 Biodiversity data

Observation type: preserved specimens

Response data type: presence only

D1.6 Predictors

Predictor types: climatic

D1.7 Hypotheses

The distribution of *O. europaea* var. *sylvestris* is limited primarily by winter cold (bio6, minimum temperature of the coldest month) and summer heat (bio10, mean temperature of the warmest quarter), with precipitation (bio18, bio12, bio15) as secondary constraints. Cold tolerance sets the cool or northern limit; heat and summer water availability set the warm or southern limit.

D1.8 Assumptions

Model assumptions: occurrence records approximate a representative sample of the species' realised distribution; the six retained predictors capture the dominant climatic constraints; the species–climate relationship is stable and transferable to future conditions (niche conservatism); climate is the primary driver of distribution at this extent (climate-only model adopted by design).

D1.9 Algorithms

Modelling techniques: multi-algorithm (MaxEnt, GLM, GAM) ensemble modelling framework, implemented via biomod2.

Model complexity: predictor set reduced to six ecologically relevant, low-collinearity variables to limit overfitting and improve transferability; single models are configured with internal package defaults.

Model averaging: yes, suitability averaged across 10 cross-validation replicates; with an ensemble model (EM) constructed by combining single models based on different algorithms.

D1.10 Workflow

Model workflow: compile occurrences (GBIF + herbaria) → clean and verify wild, non-cultivated records → assemble 19 WorldClim variables → clip to study area → reduce dimensionality via Pearson correlation ($|r| < 0.75$), and ecological relevance → retain six predictors → calibrate multi-algorithm single models with data partitioning → fit MaxEnt, GLM, and GAM (10 cross-validated replicates, 75/25 train/test) → evaluate single models using TSS and AUC on validation data → build ensemble model → project suitability maps (0–1000) for current and four future scenarios → reclassify into five classes → compute area per class in R (terra).

D1.11 Software

MaxEnt v3.4.4; R v4.5.1 with biomod2 (v4.3-4-6) and terra (v1.8-60); RStudio v2025.5.1.513; QGIS v3.40.8

Code availability: available from the corresponding author on request.

Data availability: https://doi.org/10.15468/dl.43hy77

D2 Data

D2.1 Biodiversity data

Taxon names: *Olea europaea* subsp. *europaea* var. *sylvestris* (Mill.) Lehr. Synonyms searched in GBIF: *O. sylvestris* Mill., *O. europaea* subsp. *sylvestris* (Mill.) Rouy, *O. europaea* subsp. *sylvestris* (Mill.) Rouy ex Hegi, *O. europaea* subsp. *europaea*.

Taxonomic reference system: POWO (2025), Plants of the World Online; nomenclature also follows Flora Iberica (Vargas and Talavera, 2012). Note that var. *sylvestris* is currently treated as a synonym of subsp. *europaea* in POWO.

Ecological level: species

Data sources: GBIF occurrence download (https://doi.org/10.15468/dl.43hy77, accessed 3 April 2025), plus 13 regional Mediterranean herbaria identified via Index Herbariorum, coordinated through the MGC Herbarium, University of Málaga.

Sampling design: presence only; no structured spatial or temporal sampling design; aggregated specimen records.

Sample size: 558

Clipping: Mediterranean Basin, defined by Olson et al. (2001) with modifications (small part of north-west Spain added, Canary Islands excluded).

Scaling: no spatial thinning applied, a deliberate choice to retain all available data; coordinates estimated from locality descriptions where missing; all records checked for spatial accuracy in QGIS.

Cleaning: preserved herbarium specimens only (observational records excluded); each record verified as wild, non-cultivated using locality, habitat, and collection notes; botanical garden and cultivated records excluded; duplicates between herbarium and GBIF data removed; records georeferenced and verified against the study area boundary.

Absence data: none

Background data: a single pool of 10 000 pseudo-absences randomly generated across the study area extent and shared by all three algorithms (GLM, GAM, MaxEnt); random background, no target-group bias correction.

Errors and biases: taxonomic uncertainty (var. *sylvestris* frequently recorded only as *O. europaea*, compounded by synonym and by hybridisation with cultivated olives); spatial clustering and sampling bias towards well-surveyed sites; georeferencing uncertainty for locality-estimated coordinates; severe under-sampling in the eastern Mediterranean (Türkiye, Levant, Algeria, Tunisia).

D2.2 Data partitioning

Training data: 75 % of occurrence records per replicate, used for model fitting; 10 cross-validated replicates.

Validation data: 25 % withheld per cross-validation replicate, used to estimate AUC and TSS and to average performance across replicates.

Test data: none; no spatially or fully independent external test dataset was used.

D2.3 Predictor variables

Six bioclimatic variables were retained from an initial set of 19 (bio1 to bio19): bio2 (mean diurnal range), bio6 (minimum temperature of the coldest month), bio10 (mean temperature of the warmest quarter), bio12 (annual precipitation), bio15 (precipitation seasonality), bio18 (precipitation of the warmest quarter).

Data sources: WorldClim v2.1 (Fick and Hijmans, 2017); historical climatology 1970–2000; 30 arcsec.

Spatial extent: −13.45, 44.92, 27.01, 45.98 (xmin, xmax, ymin, ymax)

Spatial resolution: 30 arcsec (∼ 1 km)

Coordinate reference system: EPSG:4326 (WGS 84) for modelling and projection; reprojected to a cylindrical equal-area projection for area calculation.

Temporal extent: 1970–2000

Data processing: all 19 variables clipped to the study area with the QGIS translate tool; no transformation or normalisation applied (handled internally by biomod2).

Dimension reduction: Pearson correlation with $|r| < 0.75$ used to drop one variable from each collinear pair (Fig. A1).

D2.4 Transfer data

Data sources: WorldClim v2.1 future projections, CMIP6 model EC-Earth3-Veg (Döscher et al., 2022), scenarios SSP2–4.5 and SSP5–8.5; 30 arcsec.

Spatial extent: –13.45, 44.92, 27.01, 45.98 (xmin, xmax, ymin, ymax)

Spatial resolution: 30 arcsec (∼ 1 km)

Temporal extent: 2041–2060 and 2061–2080

Models and scenarios: CMIP6 EC-Earth3-Veg; SSP2–4.5 and SSP5–8.5

D2.5 Model

Multicollinearity: Pearson correlation among the 19 bioclimatic variables, computed in R; pairs with $|r| > 0.75$ were considered collinear and one variable from each pair was removed, leaving six low-collinearity predictors (Fig. A1).

D2.6 Model settings

- *biomod2 single models:* multiple algorithms executed simultaneously using the BIOMOD_Modeling function. Modelling options configured under default parameters for each algorithm.
- *Ensemble settings:* built using BIOMOD_EnsembleModeling. Individual models were selected and weighted based on their validation performance scores. Projections were scaled to a continuous score between 0 and 1000.

D2.7 Model estimates

Coefficients: variable influence was assessed via randomised permutation importance across single algorithms (Table 1; bio6 dominant at 64.9) and by response curves (Fig. 2). Final predictor selection was based on the Pearson correlation analysis and ecological relevance.

D2.8 Analysis and correction of non-independence

Spatial autocorrelation: spatial autocorrelation in residuals was not explicitly modelled or corrected, and occurrences were not spatially thinned. The spatial clustering of records is acknowledged as a source of sampling bias that can inflate suitability near well-surveyed sites (Anderson and Raza, 2010; Fourcade et al., 2014).

D2.9 Threshold selection

Predictions were not converted to a strict binary presence/absence map. The continuous suitability output (0–1000) was reclassified into five equal-interval categorical suitability classes for presentation and comparison:

1. *Unsuitable: 0–200 (0–0.2)*
2. *Low: 200–400 (0.2–0.4)*
3. *Moderate: 400–600 (0.4–0.6)*
4. *High: 600–800 (0.6–0.8)*
5. *Very high: 800–1000 (0.8–1)*

D3 Assessment

D3.1 Performance statistics

Performance on training data: true skill statistic (TSS) and receiver operating characteristic (AUCroc) metric

Performance on validation data: true skill statistic (TSS) and receiver operating characteristic (AUCroc) metric

Performance on test data: none (no independent test dataset used)

D3.2 Plausibility check

Response shapes: response curves for all six predictors inspected for ecological plausibility, using ensemble response curves (Fig. 2).

Expert judgement: predicted suitability maps compared visually against the known distribution of wild olive; variable responses checked against known ecology (cold limitation via bio6, summer heat limitation via bio10).

D4 Prediction

D4.1 Prediction output

Prediction unit: per-grid-cell continuous suitability scaled from 0 to 1000 at $\sim$ 1 km resolution.

D4.2 Uncertainty quantification

Scenario uncertainty: bracketed by running two emission scenarios (SSP2–4.5 and SSP5–8.5) across two time periods.

Novel environments: clamping was applied during projection, so predictions in areas where future climate falls outside the training range are constrained to the limits of the training data. Novel environments were not separately mapped or masked from the final projections.

Code and data availability. The occurrence data include (1) GBIF herbarium specimen records filtered and cleaned from the GBIF occurrence download https://doi.org/10.15468/dl.43hy77 (GBIF.org, 2025) and (2) additional herbarium specimen records provided directly by contributing herbaria. For herbarium records obtained directly from institutions, we can share the processed data necessary to reproduce the analyses (coordinates and minimal metadata) upon request, as these records were provided by third-party institutions and are not ours to redistribute publicly.

The climatic predictors are third-party data. Current bioclimatic variables are from WorldClim v2.1 (30 arcsec; 1970–2000; Fick and Hijmans, 2017). Future bioclimatic projections for SSP2–4.5 and SSP5–8.5 based on the CMIP6 model EC-Earth3-Veg (Döscher et al., 2022) were obtained from WorldClim v2.1 at 30 arcsec spatial resolution for the periods 2041–2060 and 2061–2080. The Mediterranean Basin boundary was based on Olson et al. (2001) with the modifications described in Sect. 2.1.

All software used is publicly available, including MaxEnt v3.4.4 (Phillips et al., 2025), R (R Core Team, 2025) with the terra package (https://cran.r-project.org/package=terra, Hijmans, 2025) and biomod2 package (https://biomodhub.github.io/biomod2/, Guéguen et al., 2026), RStudio (Posit Team, 2025), and QGIS (QGIS Association, 2025).

Supplement. The supplement related to this article is available online at https://doi.org/10.5194/we-26-251-2026-supplement.

Author contributions. WZ contributed to conceptualisation of the study, conducted the analyses, curated and processed the data, generated the figures, and wrote the original draft of the paper. NH-T coordinated the conceptualisation of the study, contributed to study design and methodology, provided supervision and project administration, facilitated access to resources, and critically reviewed and edited the paper. AS-T contributed to the analyses, figures, and cartographic resources; provided guidance on analytical tools; and critically reviewed and edited the paper. All authors approved the final version of the article.

Competing interests. The contact author has declared that none of the authors has any competing interests.

Disclaimer. Publisher's note: Copernicus Publications remains neutral with regard to jurisdictional claims made in the text, published maps, institutional affiliations, or any other geographical representation in this paper. The authors bear the ultimate responsibility for providing appropriate place names. Views expressed in the

text are those of the authors and do not necessarily reflect the views of the publisher.

Acknowledgements. We thank José García Sánchez of the MGC Herbarium (University of Málaga) for facilitating contact with the herbaria consulted for distribution data. We also thank the herbaria and their staff for providing access to occurrence records and for their assistance with enquiries during this study. We are grateful to the following institutions: Università di Siena, the Hebrew University of Jerusalem Herbarium, Universidad de Jaén, Universidad de Almería, the Jardí Botànic de Sóller, the University of Camerino Herbarium, the Goulandris Natural History Museum, the Aix-Marseille Université Herbarium, the Università degli Studi di Cagliari, the Museu Nacional de História Natural e da Ciência (University of Lisbon), the Universidad de Córdoba, the Universidad de León, and the University of Barcelona Herbarium (CEDOCBIV).

Review statement. This paper was edited by Merin Reji Chacko and reviewed by two anonymous referees.

References

Alegria, C., Almeida, A. M., Roque, N., Fernandez, P., and Ribeiro, M. M.: Species distribution modelling under climate change scenarios for maritime pine (*Pinus pinaster Aiton*) in Portugal, Forests, 14, 591, https://doi.org/10.3390/f14030591, 2023.

Allouche, O., Tsoar, A., and Kadmon, R.: Assessing the accuracy of species distribution models: prevalence, kappa and the true skill statistic (TSS), J. Appl. Ecol., 43, 1223–1232, https://doi.org/10.1111/j.1365-2664.2006.01214.x, 2006.

Anderson, R. P. and Raza, A.: The effect of the extent of the study region on GIS models of species geographic distributions and estimates of niche evolution: preliminary tests with montane rodents (genus Nephelomys) in Venezuela, J. Biogeogr., 37, 1378–1393, https://doi.org/10.1111/j.1365-2699.2010.02290.x, 2010.

Arenas-Castro, S., Gonçalves, J. F., Moreno, M., and Villar, R.: Projected climate changes are expected to decrease the suitability and production of olive varieties in southern Spain, Sci. Total Environ., 709, 136161, https://doi.org/10.1016/j.scitotenv.2019.136161, 2020.

Ben-Dor, E., Dag, A., Perelberg, A., Chen, T., Ben Dor, Y., Low Ramati, D., Tietel, Z., Galili, E., Heinze, B., and Barazani, O.: Genetic and phenotypic evidence suggest the existence of indigenous olive population of wild var. *sylvestris* in the Carmel coast, southern Levant, BMC Plant Biol., 24, 896, https://doi.org/10.1186/s12870-024-05575-7, 2024.

Besnard, G., Khadari, B., Navascués, M., Fernández-Mazuecos, M., El Bakkali, A., Arrigo, N., Baali-Cherif, D., Brunini-Bronzini de Caraffa, V., Santoni, S., Vargas, P., and Savolainen, V.: The complex history of the olive tree: from Late Quaternary diversification of Mediterranean lineages to primary domestication in the northern Levant, P. Roy. Soc. B-Biol. Sci., 280, 20122833, https://doi.org/10.1098/rspb.2012.2833, 2013.

Besnard, G., Terral, J. F., and Cornille, A.: On the origins and domestication of the olive: a review and perspectives, Ann. Bot., 121, 385–403, https://doi.org/10.1093/aob/mcx145, 2018.

Cramer, W., Guiot, J., and Marini, K.: Climate and environmental change in the Mediterranean Basin: current situation and risks for the future, First Mediterranean Assessment Report, Union for the Mediterranean, Plan Bleu, Zenodo, https://doi.org/10.5281/zenodo.4768833, 2020.

Curtis, S.: Means and long-term trends of global coastal zone precipitation, Sci. Rep., 9, 5401, https://doi.org/10.1038/s41598-019-41878-8, 2019.

Dimopoulos, P., Raus, T., Bergmeier, E., Constantinidis, T., Iatrou, G., Kokkini, S., Strid, A., and Tzanoudakis, D.: Vascular plants of Greece: an annotated checklist. Supplement, Willdenowia, 46, 301–347, https://doi.org/10.3372/wi.46.46303, 2016.

Dormann, C. F., Elith, J., Bacher, S., Buchmann, C., Carl, G., Carré, G., Marquéz, J. R. G., Gruber, B., Lafourcade, B., Leitão, P. J., Münkemüller, T., McClean, C., Osborne, P. E., Reineking, B., Schröder, B., Skidmore, A. K., Zurell, D., and Lautenbach, S.: Collinearity: a review of methods to deal with it and a simulation study evaluating their performance, Ecography, 36, 27–46, https://doi.org/10.1111/j.1600-0587.2012.07348.x, 2013.

Döscher, R., Acosta, M., Alessandri, A., Anthoni, P., Arsouze, T., Bergman, T., Bernardello, R., Boussetta, S., Caron, L.-P., Carver, G., Castrillo, M., Catalano, F., Cvijanovic, I., Davini, P., Dekker, E., Doblas-Reyes, F. J., Docquier, D., Echevarria, P., Fladrich, U., Fuentes-Franco, R., Gröger, M., v. Hardenberg, J., Hieronymus, J., Karami, M. P., Keskinen, J.-P., Koenigk, T., Makkonen, R., Massonnet, F., Ménégoz, M., Miller, P. A., Moreno-Chamarro, E., Nieradzik, L., van Noije, T., Nolan, P., O'Donnell, D., Ollinaho, P., van den Oord, G., Ortega, P., Prims, O. T., Ramos, A., Reerink, T., Rousset, C., Ruprich-Robert, Y., Le Sager, P., Schmith, T., Schrödner, R., Serva, F., Sicardi, V., Sloth Madsen, M., Smith, B., Tian, T., Tourigny, E., Uotila, P., Vancoppenolle, M., Wang, S., Wårlind, D., Willén, U., Wyser, K., Yang, S., Yepes-Arbós, X., and Zhang, Q.: The EC-Earth3 Earth system model for the Coupled Model Intercomparison Project 6, Geosci. Model Dev., 15, 2973–3020, https://doi.org/10.5194/gmd-15-2973-2022, 2022.

Elith, J., Phillips, S. J., Hastie, T., Dudík, M., Chee, Y. E., and Yates, C. J.: A statistical explanation of MaxEnt for ecologists, Divers. Distrib., 17, 43–57, https://doi.org/10.1111/j.1472-4642.2010.00725.x, 2011.

El-Samra, R., Bou-Zeid, E., Bangalath, H. K., Stenchikov, G., and El-Fadel, M.: Seasonal and regional patterns of future temperature extremes: high-resolution dynamic downscaling over a complex terrain, J. Geophys. Res.-Atmos., 123, 6669–6689, https://doi.org/10.1029/2017JD027500, 2018.

Fanelli, V., Mascio, I., Falek, W., Miazzi, M. M., and Montemurro, C.: Current status of biodiversity assessment and conservation of wild olive (*Olea europaea* L. subsp. *europaea* var. *sylvestris*), Plants, 11, 480, https://doi.org/10.3390/plants11040480, 2022.

Fick, S. E. and Hijmans, R. J.: WorldClim 2: new 1 km spatial resolution climate surfaces for global land areas, Int. J. Climatol., 37, 4302–4315, https://doi.org/10.1002/joc.5086, 2017.

Fielding, A. H. and Bell, J. F.: A review of methods for the assessment of prediction errors in conservation presence/absence models, Environ. Conserv., 24, 38–49, https://doi.org/10.1017/S0376892997000088, 1997.

Filahi, H., Omrani, H., Drobinski, P., Claudel, S., and Oueslati, B.: Selecting CMIP6 models to assess the impact of climate change on energy need for heating and cooling in Europe, Theor. Appl. Climatol., 156, 126, https://doi.org/10.1007/s00704-024-05263-4, 2025.

Fourcade, Y., Engler, J. O., Rödder, D., and Secondi, J.: Mapping species distributions with MaxEnt using a geographically biased sample of presence data: a performance assessment of methods for correcting sampling bias, PLoS One, 9, e97122, https://doi.org/10.1371/journal.pone.0097122, 2014.

Fraga, H., Guimarães, N., Freitas, T. R., Malheiro, A. C., and Santos, J. A.: Future scenarios for olive tree and grapevine potential yields in the World Heritage Côa region, Portugal, Agronomy, 12, 350, https://doi.org/10.3390/agronomy12020350, 2022.

Fuss, S., Canadell, J. G., Peters, G. P., Tavoni, M., Andrew, R. M., Ciais, P., Jackson, R. B., Jones, C. D., Kraxner, F., Nakicenovic, N., Le Quéré, C., Raupach, M. R., Sharifi, A., Smith, P., and Yamagata, Y.: Betting on negative emissions, Nat. Clim. Change, 4, 850–853, https://doi.org/10.1038/nclimate2392, 2014.

GBIF: Global Biodiversity Information Facility, https://www.gbif.org/what-is-gbif (last access: 3 April 2025), 2025.

GBIF.org: GBIF Occurrence Download, GBIF [data set], https://doi.org/10.15468/dl.43hy77 (last access: 3 April 2025), 2025.

Gritti, E. S., Smith, B., and Sykes, M. T.: Vulnerability of Mediterranean Basin ecosystems to climate change and invasion by exotic plant species, J. Biogeogr., 33, 145–157, https://doi.org/10.1111/j.1365-2699.2005.01377.x, 2006.

Guéguen, M., Blancheteau, H., Lemaire-Patin, R., and Thuiller, W.: biomod2: Ensemble Platform for Species Distribution Modeling, R package version 4.3-4-6, CRAN [code], https://CRAN.R-project.org/package=biomod2 (last access: 25 June 2026), 2026.

Guerrero Maldonado, N., López, M. J., Caudullo, G., and de Rigo, D.: *Olea europaea* in Europe: distribution, habitat, usage and threats, in: European Atlas of Forest Tree Species, edited by: San-Miguel-Ayanz, J., de Rigo, D., Caudullo, G., Houston Durrant, T., and Mauri, A., Publications Office of the European Union, Luxembourg, e01534b+, ISBN 978-92-76-17290-1, https://doi.org/10.2760/776635, 2016.

Gulev, S. K., Thorne, P. W., Ahn, J., Dentener, F. J., Domingues, C. M., Gerland, S., Gong, D., Kaufman, D. S., Nnamchi, H. C., Quaas, J., Rivera, J. A., Sathyendranath, S., Smith, S. L., Trewin, B., von Schuckmann, K., and Vose, R. S.: Changing state of the climate system, in: Climate Change 2021: The Physical Science Basis. Contribution of Working Group I to the Sixth Assessment Report of the Intergovernmental Panel on Climate Change, edited by: Masson-Delmotte, V., Zhai, P., Pirani, A., Connors, S. L., Péan, C., Berger, S., Caud, N., Chen, Y., Goldfarb, L., Gomis, M. I., Huang, M., Leitzell, K., Lonnoy, E., Matthews, J. B. R., Maycock, T. K., Waterfield, T., Yelekçi, O., Yu, R., and Zhou, B., Cambridge University Press, Cambridge, 287–422, https://doi.org/10.1017/9781009157896.001, 2021.

Haworth, M., Marino, G., Brunetti, C., Killi, D., De Carlo, A., and Centritto, M.: The impact of heat stress and water deficit on the photosynthetic and stomatal physiology of olive (*Olea europaea* L.): a case study of the 2017 heat wave, Plants, 7, 76, https://doi.org/10.3390/plants7040076, 2018.

Hidalgo-Triana, N., Solakis, A., Casimiro-Soriguer, F., Choe, H., Navarro, T., Pérez-Latorre, A. V., and Thorne, J. H.: The high climate vulnerability of western Mediterranean forests, Sci. Total Environ., 895, 164983, https://doi.org/10.1016/j.scitotenv.2023.164983, 2023.

Hijmans, R. J.: terra: spatial data analysis (version 1.8-60), CRAN [code], https://cran.r-project.org/package=terra (last access: 5 July 2025), 2025.

Kassout, J., Terral, J. F., El Ouahrani, A., Houssni, M., Ivorra, S., Kadaoui, K., El Mahroussi, M., Paradis, L., and Ater, M.: Species distribution based-modelling under climate change: the case of two native wild *Olea europaea* subspecies in Morocco, O. e. subsp. *europaea* var. *sylvestris* and O. e. subsp. *maroccana*, in: Climate change in the Mediterranean and Middle Eastern region, edited by: Leal Filho, W. and Manolas, E., Springer International Publishing, Cham, 21–43, https://doi.org/10.1007/978-3-030-78566-6_2, 2022.

Khan, A. M., Li, Q., Saqib, Z., Khan, N., Habib, T., Khalid, N., Majeed, M., and Tariq, A.: MaxEnt modelling and impact of climate change on habitat suitability variations of economically important Chilgoza pine (*Pinus gerardiana* Wall.) in South Asia, Forests, 13, 715, https://doi.org/10.3390/f13050715, 2022.

Li, Y., Li, M., Li, C., and Liu, Z.: Optimized MaxEnt model predictions of climate change impacts on the suitable distribution of *Cunninghamia lanceolata* in China, Forests, 11, 302, https://doi.org/10.3390/f11030302, 2020.

Luque Söllheim, Á. L., Máyer Suarez, P., and García Hernández, F.: The digital climate atlas of the Canary Islands: a tool to improve knowledge of climate and temperature and precipitation trends in the Atlantic islands, Climate Services, 34, 100487, https://doi.org/10.1016/j.cliser.2024.100487, 2024.

McPherson, J. M. and Jetz, W.: Effects of species' ecology on the accuracy of distribution models, Ecography, 30, 135–151, https://doi.org/10.1111/j.0906-7590.2007.04823.x, 2007.

Médail, F. and Quézel, P.: Biodiversity hotspots in the Mediterranean Basin: setting global conservation priorities, Conserv. Biol., 13, 1510–1513, https://doi.org/10.1046/j.1523-1739.1999.98467.x, 1999.

Menezes-Silva, P. E., Loram-Lourenço, L., Alves, R. D. F. B., Sousa, L. F., Almeida, S. E. S., and Farnese, F. S.: Different ways to die in a changing world: consequences of climate change for tree species performance and survival through an ecophysiological perspective, Ecol. Evol., 9, 11979–11999, https://doi.org/10.1002/ece3.5663, 2019.

Miller, J.: Species distribution modeling, Geography Compass, 4, 490–509, https://doi.org/10.1111/j.1749-8198.2010.00351.x, 2010.

Nelder, J. A. and Wedderburn, R. W. M.: Generalized linear models, J. R. Stat. Soc. A Gen., 135, 370–384, https://doi.org/10.2307/2344614, 1972.

O'Neill, B. C., Tebaldi, C., van Vuuren, D. P., Eyring, V., Friedlingstein, P., Hurtt, G., Knutti, R., Kriegler, E., Lamarque, J.-F., Lowe, J., Meehl, G. A., Moss, R., Riahi, K., and Sanderson, B. M.: The Scenario Model Intercomparison Project (ScenarioMIP) for CMIP6, Geosci. Model Dev., 9, 3461–3482, https://doi.org/10.5194/gmd-9-3461-2016, 2016.

Olson, D. M., Dinerstein, E., Wikramanayake, E. D., Burgess, N. D., Powell, G. V. N., Underwood, E. C., D'Amico, J. A., Itoua, I., Strand, H. E., Morrison, J. C.,

Loucks, C. J., Allnutt, T. F., Ricketts, T., Kura, Y., Lamoreux, J., Wettengel, W. W., Hedao, P., and Kassem, K.: Terrestrial ecoregions of the world: a new map of life on Earth, BioScience, 51, 933–938, https://doi.org/10.1641/0006-3568(2001)051[0933:TEOTWA]2.0.CO;2, 2001.

Özdel, M. M., Ustaoğlu, B., and Cürebal, İ.: Climate-driven futures of olive (*Olea europaea* L.): machine learning-based ensemble species distribution modelling of northward shifts under aridity stress, Plants, 14, 3774, https://doi.org/10.3390/plants14243774, 2025.

Pecl, G. T., Araújo, M. B., Bell, J. D., Blanchard, J., Bonebrake, T. C., Chen, I. C., Clark, T. D., Colwell, R. K., Danielsen, F., Evengård, B., Falconi, L., Ferrier, S., Frusher, S., Garcia, R. A., Griffis, R. B., Hobday, A. J., Janion-Scheepers, C., Jarzyna, M. A., Jennings, S., Lenoir, J., Linnetved, H. I., Martin, V. Y., McCormack, P. C., McDonald, J., Mitchell, N. J., Mustonen, T., Pandolfi, J. M., Pettorelli, N., Popova, E., Robinson, S. A., Scheffers, B. R., Shaw, J. D., Sorte, C. J. B., Strugnell, J. M., Sunday, J. M., Tuanmu, M. N., Vergés, A., Villanueva, C., Wernberg, T., Wapstra, E., and Williams, S. E.: Biodiversity redistribution under climate change: impacts on ecosystems and human well-being, Science, 355, eaai9214, https://doi.org/10.1126/science.aai9214, 2017.

Petruccelli, R., Bartolini, G., Ganino, T., Zelasco, S., Lombardo, L., Perri, E., Durante, M., and Bernardi, R.: Cold stress, freezing adaptation, varietal susceptibility of *Olea europaea* L.: a review, Plants, 11, 1367, https://doi.org/10.3390/plants11101367, 2022.

Phillips, S. J., Anderson, R. P., and Schapire, R. E.: Maximum entropy modeling of species geographic distributions, Ecol. Model., 190, 231–259, https://doi.org/10.1016/j.ecolmodel.2005.03.026, 2006.

Phillips, S. J., Dudík, M., and Schapire, R. E.: MaxEnt software for modeling species niches and distributions (version 3.4.4), American Museum of Natural History [code], http://biodiversityinformatics.amnh.org/open_source/maxent/ (last access: 10 April 2025), 2025.

Posit Team: RStudio: integrated development environment for R (version 2025.5.1.513), Posit Software [code], PBC, Boston, http://www.posit.co/ (last access: 20 May 2025), 2025.

Pontius, R. G. and Parmentier, B.: Recommendations for using the relative operating characteristic (ROC), Landsc. Ecol., 29, 367–382, https://doi.org/10.1007/s10980-013-9984-8, 2014.

POWO: Plants of the World Online. World Checklist of Vascular Plants, facilitated by the Royal Botanic Gardens, Kew, https://powo.science.kew.org (last access: 3 September 2025), 2025.

QGIS Association: QGIS geographic information system (version 3.40.8), http://www.qgis.org (last access: 23 April 2025), 2025.

R Core Team: R: the R Project for Statistical Computing (version 4.5.1), https://www.r-project.org/ (last access: 15 June 2025), 2025.

Rubenstein, M. A., Weiskopf, S. R., Bertrand, R., Carter, S. L., Comte, L., Eaton, M. J., Johnson, C. G., Lenoir, J., Lynch, A. J., Miller, B. W., Morelli, T. L., Rodriguez, M. A., Terando, A., and Thompson, L. M.: Climate change and the global redistribution of biodiversity: substantial variation in empirical support for expected range shifts, Environmental Evidence, 12, 7, https://doi.org/10.1186/s13750-023-00296-0, 2023.

Ruiz, N., Barranco, D., and Rapoport, H. F.: Anatomical response of olive (*Olea europaea* L.) to freezing temperatures, J. Hortic. Sci. Biotech., 81, 783–790, https://doi.org/10.1080/14620316.2006.11512138, 2006.

Sweetgum: Index Herbariorum, New York Botanical Garden, https://sweetgum.nybg.org/science/ih/ (last access: 5 May 2025), 2025.

Tsiftsis, S., Mastrogianni, A., Kiziridis, D. A., Xystrakis, F., Pleniou, M., and Tsiripidis, I.: Land-use changes largely determine the trajectory of plant species distributions under climatic uncertainty in a Mediterranean landscape, Land, 14, 1438, https://doi.org/10.3390/land14071438, 2025.

Valavi, R., Guillera-Arroita, G., Lahoz-Monfort, J. J., and Elith, J.: Predictive performance of presence-only species distribution models: a benchmark study with reproducible code, Ecol. Monogr., 91, e01486, https://doi.org/10.1002/ecm.1486, 2021.

Vargas, P. and Talavera, S.: *Olea*, in: Flora Iberica XI. Gentianaceae–Boraginaceae, edited by: Talavera, S., Andrés, C., Arista, M., Fernández Piedra, M. P., Gallego, M. J., Ortiz, P. L., Romero Zarco, C., Salgueiro, F. J., Silvestre, S., Quintanar, A., Castroviejo, S., Real Jardín Botánico, CSIC, Madrid, 136–139, http://www.floraiberica.es/ (last access: 8 May 2025), 2012.

Wood, S. N.: Generalized Additive Models: An Introduction with R, 2nd edn., Chapman and Hall/CRC Texts in Statistical Science, CRC Press/Taylor & Francis Group, Boca Raton, 496 pp., https://doi.org/10.1201/9781315370279, 2017.

Zurell, D., Franklin, J., König, C., Bouchet, P. J., Serra-Diaz, J. M., Dormann, C. F., Elith, J., Fandos Guzman, G., Feng, X., Guillera-Arroita, G., Guisan, A., Leitão, P. J., Lahoz-Monfort, J. J., Park, D. S., Peterson, A. T., Rapacciuolo, G., Schmatz, D. R., Schröder, B., Thuiller, W., Yates, K. L., Zimmermann, N. E., and Merow, C.: A standard protocol for describing species distribution models, Ecography, 43, 1261–1277, https://doi.org/10.1111/ecog.04960, 2020.